AI-CE-42
METALS, CERAMICS, AND
MATERIALS

# HEAVY WATER
# ORGANIC COOLED REACTOR

## LONG-TERM STRESS-RUPTURE PROPERTIES
## OF FINNED SAP CLADDING TUBES

By

P. B. FERRY
D. N. GLASS



Contract: AT(38-1)-430
FOR THE
U.S. ATOMIC ENERGY COMMISSION

ISSUED: SEPTEMBER 25, 1967

ATOMICS INTERNATIONAL—COMBUSTION ENGINEERING
A Joint Venture for Heavy Water Organic Cooled Reactors

## DISCLAIMER

## DISTRIBUTION

This report has been distributed according to the category "Metals, Ceramics, and Materials" as given in the Standard Distribution for Unclassified Scientific and Technical Reports, TID-4500.

## CONTENTS



## TABLES

## FIGURES

# I. INTRODUCTION

Organic cooled, heavy water moderated reactors offer an attractive concept for producing low-cost power. In a concept such as the Heavy Water Organic Cooled Reactor (HWOCR), it is planned to use either low enriched or natural uranium as a fissile fuel. Because of this, it is necessary to use a low thermal neutron capture cross-section material for the structural in-core components. Sintered aluminum powder (SAP) alloys combine the attractive thermal and nuclear characteristics of aluminum with useful strength at organic coolant temperatures. These alloys have been chosen as reference material for HWOCR pressure tube and fuel cladding applications.

The SAP alloys are powder metallurgy products of commercially pure aluminum with additions of $Al_2O_3$ as a stable dispersion-strengthening agent. Comparison of reported mechanical properties data indicates that differences in material lots, fabrication histories, and testing methods cause an inordinate amount of scatter in the test data.

Extensive mechanical testing of these alloys has heretofore been primarily limited to short-term uniaxial and biaxial stress tests and long-term uniaxial tests. There has been a limited amount of long-term testing in the biaxial stress state by Fleming[1] but this has been limited to a relatively narrow range of stresses and temperatures.

This report describes the biaxial test facility designed and fabricated to test HWOCR fuel element cladding designs, and also the first series of tests designed to evaluate the properties of finished SAP shapes. These data were analyzed by Larson-Miller type evaluations to provide extrapolations for predicting material behavior under reactor operating conditions.

# II. METHOD OF TESTING

## A. TEST MATERIAL

The specimens for these tests were extruded at the same time and under the same conditions as the fuel cladding for the EXP-NRU-305, 305-A1, and 305-A2 irradiation experiments. A description of the experiment design and operation is described by Culley[2] and will not be included here. The materials selected included 7 and 10% SAP alloys with different fabrication histories. The identification and alloy references are shown in Table 1. The chemistry of the alloys is presented in Table 2. The lots were made in three separate extrusion runs and are separated in that manner.

TABLE 1

COMPOSITION AND FABRICATION HISTORY OF ALLOYS TESTED

| Lot Designation | Alloy | Raw Product Supplier, Billet Diameter (in.) and Date Fabricated | Fabrication Sequence** (Diameter in inches) |
|---|---|---|---|
| U 305 | XAP 001 | Alcoa,† 3-3/4, 1964 | 3-3/4 → 1-1/2 → finished finned tube |
| U 305A1 | XAP 005 | Alcoa, 3-3/4, 1964 | 3-3/4 → 1-1/2 → finished finned tube |
| U 305A1 | SAP 895* | HDA,§ 2-3/8, 1962 | 2-3/8 → 1-1/2 → finished finned tube |
| U 305A2 | XAP 001 | Alcoa, 7-3/4, 1962 | 7-3/4 → 4-1/4 → 1-1/2 → finished finned tube |
| | XAP 001 | Alcoa, 3-3/4, 1964 | 3-3/4 → 1-1/2 → finished finned tube |

*This alloy contains a nominal 10 wt % aluminum oxide. All other alloys tested contain a nominal 7 wt % aluminum oxide.
†Aluminum Company of America, Pittsburgh, Pennsylvania
§HDA = High Duty Alloys (Swiss Aluminum)
**All finishing operations were performed by Torrance Extrusion Corp., Banning, California

The finned tubing was extruded to conform to the dimensions shown in Figure 1. The extrusion process features a hollow, direct hydraulic extrusion through a conical die with billet preheat temperatures of 650 to 850°F. The post-extrusion operations included cold-twisting to produce spiralled fins (90°/ft), ball sizing to establish the close tolerances of the inside diameter, and stretch straightening. Study of the effects of extrusion ratios, preheat

TABLE 2

CHEMICAL ANALYSIS OF U-305, U-305 ALT. 1, AND U-305 ALT. 2 SAP FUEL CLADDING

| | XAP 001* | XAP 005† | XAP 001§ | Specification |
|---|---|---|---|---|
| $Al_2O_3$ | 6.31% | 6.36% | 6.86% | 2.0 to 7.0% |
| Boron | 3 | 3 | 10 | 3 |
| Calcium | 50 | 50 | 50 | 100 |
| Cadmium | 10 | 10 | 10 | 50 |
| Carbon | 0.68% | 0.54% | 0.59% | - |
| Chromium | 1 | 5 | 10 | 100 |
| Copper | 10 | 10 | 10 | 100 |
| Gallium | 50 | 50 | 50 | - |
| Iron | 500 | 500 | 1000 | 500 |
| Magnesium | 20 | 10 | 30 | 50 |
| Manganese | 5 | 5 | 10 | 100 |
| Molybdenum | 10 | 10 | 10 | 50 |
| Nickel | 10 | 10 | 10 | 100 |
| Lead | 10 | 10 | 10 | 40 |
| Silicon | 1000 | 900 | 1000 | 1000 |
| Tin | 10 | 10 | 10 | 100 |
| Titanium | 20 | 20 | 10 | 300 |
| Vanadium | 25 | 10 | 50 | - |
| Zinc | 100 | 100 | 100 | 100 |
| Zirconium | 500 | 10 | 10 | - |
| Nitrogen | 110 | 242 | 110 | 200 |
| Hydrogen | 17 | 28 | 30 | 20 |

All values listed are in ppm with the exception of $Al_2O_3$ and carbon, which are reported in wt %.

*Extruded from 3-3/4-in. — used in NRU-305 and Alt.1.
†Extruded from 3-3/4-in. — used only in Alt.1.
§Extruded from 7-3/4-in. — used in NRU 305, Alt.1 and Alt.2.

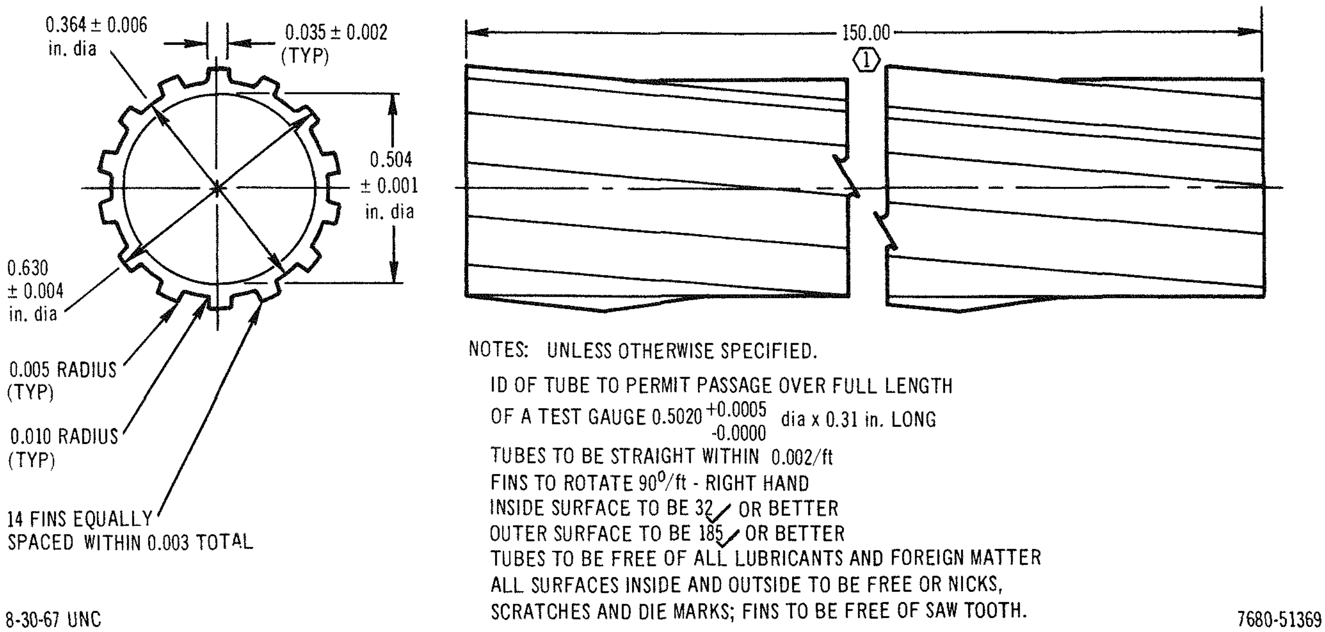


Figure 1. Dimensions of Tested Finned Tubing

temperatures, die design, and post-extrusion operations was planned for the future and was not included as part of this program.

## B. TEST APPARATUS

The design of the Mark III test rigs used in the HWOCR program was based on experience gained during development of stress-rupture rigs over the past few years. The problem areas will be noted in an effort to aid other investigators to avoid similar difficulties.

### 1. Mark I

The initial pressure stress-rupture rigs used at AI were basically a cluster of seven SAP tubes in a bolt circle connected to a common plenum by use of standard stainless steel tube fittings as shown in Figure 2. It was intended that, when a specimen ruptured, the test would be interrupted and that specimen removed. The pressure lead could then be capped off and the remaining specimens returned to test. The tube fitting joints were unaffected by pressure cycles, and the design worked adequately as long as there were no thermal cycles. Upon thermal cycling, however, the SAP tubing would contract more than the steel on cooling, and the fitting would leak. Upon reheating, the joints

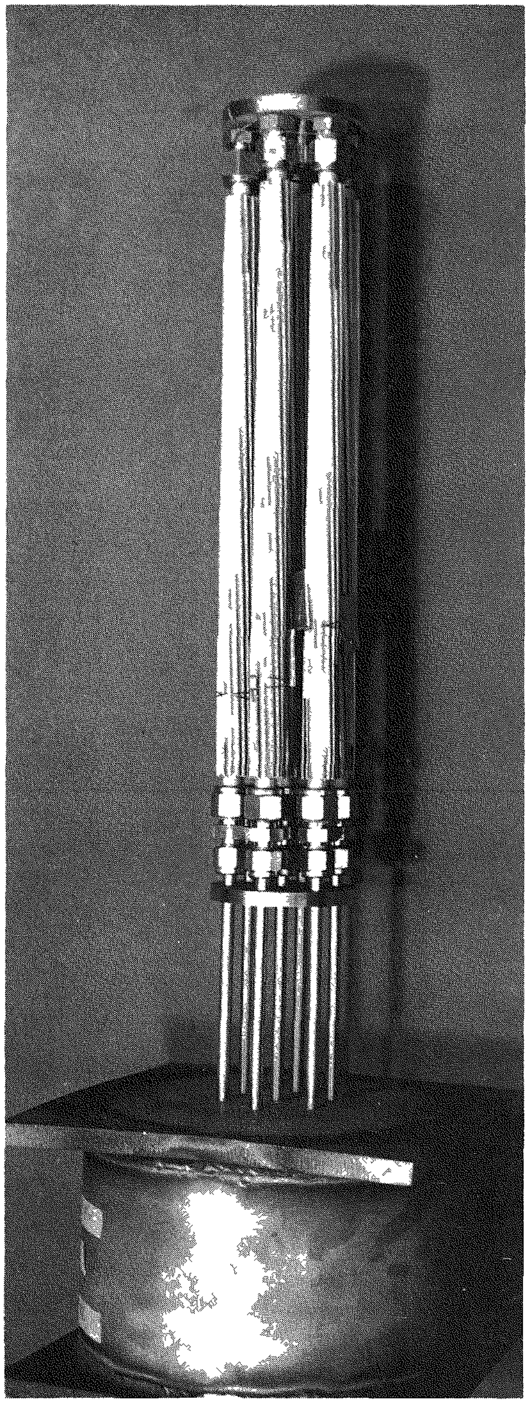

5 15 63 UNC 7500 1874

Figure 2. Mark I Test Assembly — Seven Test Specimens Sharing Common Plenum

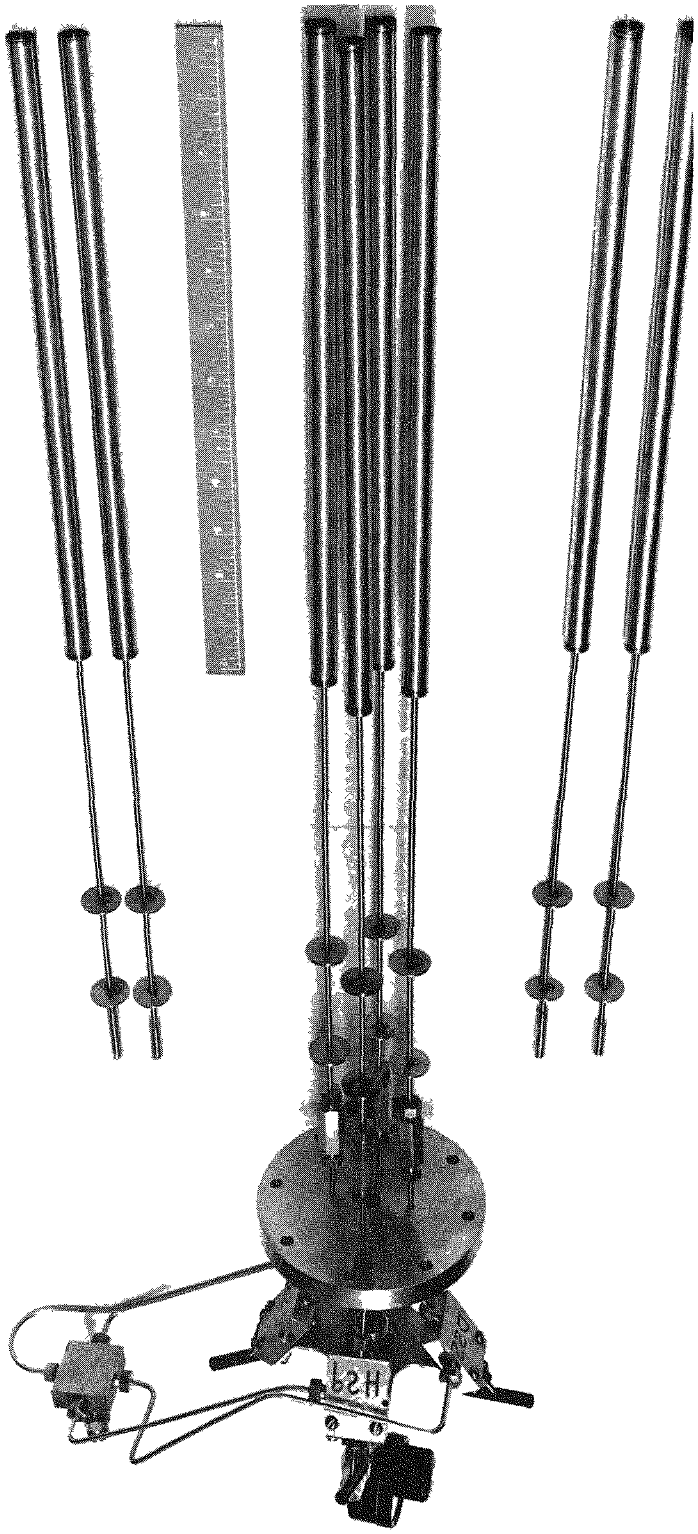

6-4-65 UNC 7661 1815

Figure 3. Specimen Configuration for Mark II Test Apparatus

would not reseal. This was attributed to the interdiffusion of the steel and SAP, forming a brittle diffusion zone which would fracture under mechanical movement. Some diffusion barriers were tried but none proved to be very satisfactory. The rigs did operate continuously in excess of 20,000 hours at test temperatures up to 900°F. The design was discontinued because of the thermal-cycle limitation.

2. Mark II

The next test style was designed for nickel- and iron-base wrought alloys. The specimen configuration is shown in Figure 3. This set-up allows individual pressurization of four separate specimens in controlled environment retorts in a single furnace. The flange separating the specimens and valves is the sealing face between the specimens and the ambient environment. All joints operating at elevated temperature are welded. The lower temperature sections are high pressure tube fittings and can be connected or disconnected for ease of plumbing. This design was used successfully for a number of years, testing over 1000 specimens of wrought alloys in such environments as sodium, NaK (internal and external), helium, argon, and vacuum (external) and undergoing many pressure and thermal cycles.

3. Mark III

The HWOCR development program required techniques for tube burst stress-rupture testing SAP shapes. The basic design of plumbing and facilities was to be the same as had been successful for wrought alloys (i.e., the Mark II system). The transition joint problem (aluminum to stainless steel) remained to be solved. Aluminum had been successfully used as end plug material to seal SAP fuel cladding tubes for short-term pressure burst tests. It is estimated that as many as 300 aluminum plugs have been tested in tube burst tests (from room temperature to 1000°F) without a single failure occurring at the end plug. Based on this experience, a number of approaches using heavy wall wrought aluminum capillary tubing were tried, (in December 1965) but without success. The aluminum tubing would not operate at temperatures in excess of 750°F for more than a few days. Further experiments established that the aluminum lead tube would work below 400°F; however, this produced an undesired thermal gradient on the specimen.

It was at this time that Jackson developed a method for a tubular transition joint between austenitic stainless steel and aluminum.[3] The design provided a compatible seal for in-rod instrumentation of fuel irradiation experiments. A detailed description of the process is reported by Jackson and will only be highlighted here. A Type 304 stainless steel tube is coated with a suitable metallic diffusion barrier. The tube is inserted into an 1100 Aluminum tube and the composite is then evacuated and welded closed. The steel is then bonded to the aluminum by the hot isostatic gas process and the composite is machined to the required end plug configuration. An example of the components and resultant joints is shown in Figure 4. The transition plug is then silver diffusion-bonded to one end of the SAP specimen, the other end being sealed with the standard blind plug. Details of the silver diffusion-bonding process are reported by Jackson.[3] A steel lead tube is joined to the transition cap by means of a partial penetration sleeve weld. The components for this are shown in Figure 5. This method not only works well, but is very simple in design and low in cost. A large number of transition joints could be prefabricated and then bonded by the normal pilot production fuel element fabrication facility. With the stainless steel lead tube, the specimen would then interface well with the facility being built of the basic Mark II design.

Details of the test assembly are shown in Figure 6. The disks and insulation on the lead tube are to minimize convection and keep the O-ring and mechanical seals and valves cool. The small steel tubes on the outside of the retorts are for thermocouples. Three thermocouples are used to monitor the temperature at the top, middle, and bottom of the retort. A fourth thermocouple is used for a secondary calibration thermocouple which can be inserted during test to monitor and correct any thermocouple drift which may occur. A mockup rig with all test components and with thermocouples both inside and outside the retort is used to determine the relationship between the monitor thermocouples and actual specimen temperature at each temperature tested and in each furnace design. (Two furnace sizes were used.) Two test assemblies are shown in Figure 7. The furnace on the left is 5-in. in diameter and capable of testing large components. The furnace on the right is 2-in. in diameter.

The gages above the test rigs are used daily to monitor the pressure in the specimens. They are plumbed directly to the lead tube of the specimens. If a

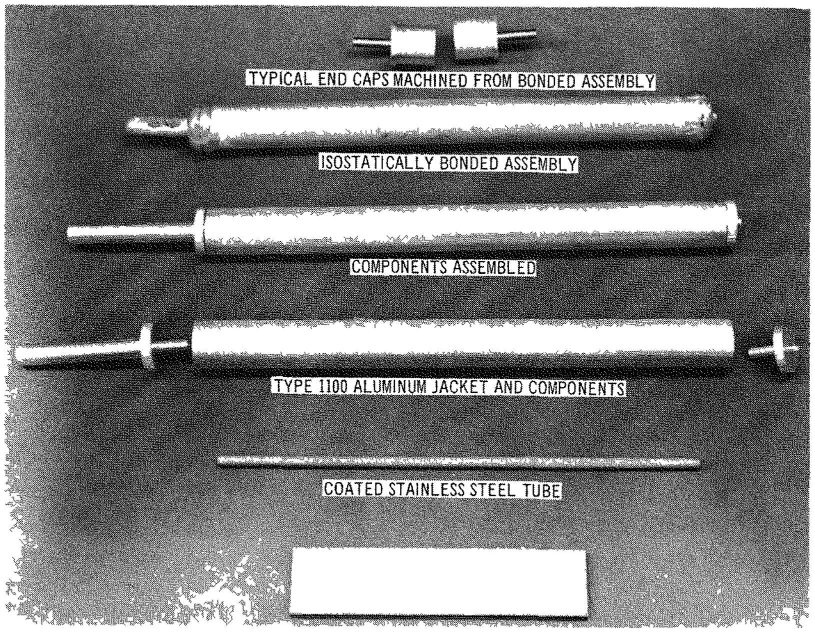


7680-4039

Figure 4. Components Illustrating Steps in Fabrication of Transition Joints

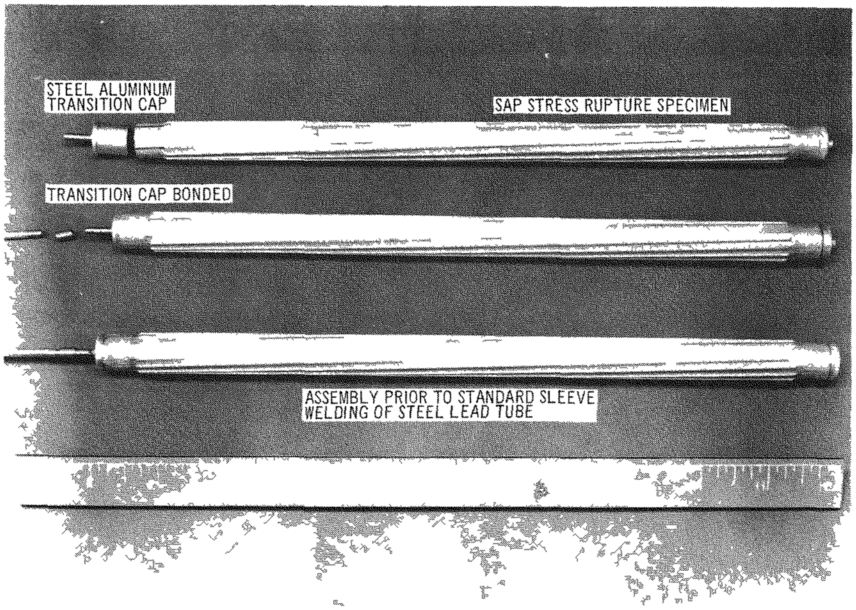


7680 4038

Figure 5 Components Illustrating Lead Tube Attachment to End Cap

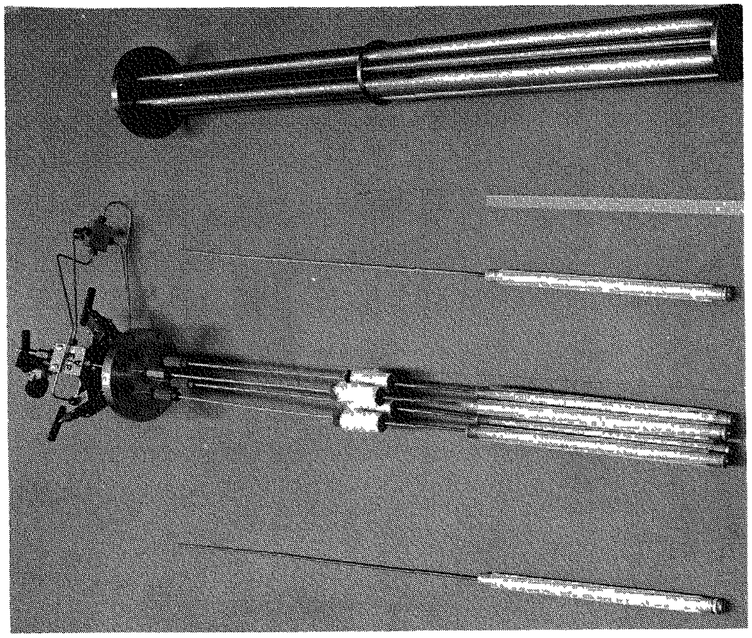

4-29-66 UNC 7680-1850

Figure 6. Test Apparatus for Mark III Test Apparatus

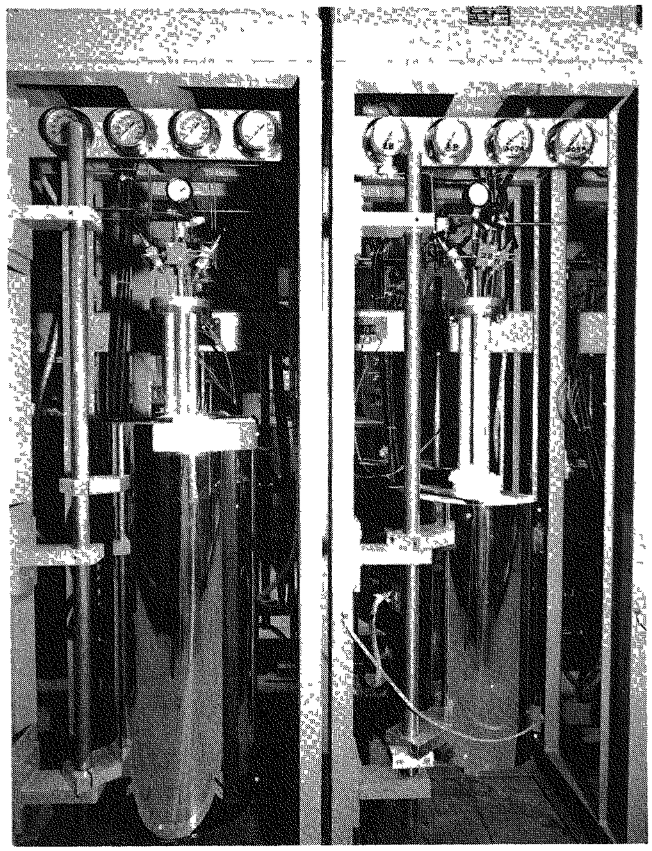

4-29-66 UNC 7680-1851

Figure 7. 5-in. (left) and 2-in. (right) Diameter Furnaces Used for Testing Tubes

specimen ruptures, or if there is a leak in the system, the pressure on this gage falls. If this is not accompanied by an increase in the indicated pressure on the retort gage, a leak in the external portion of the system is indicated. If the pressure does rise in the retort, that specimen indicating a pressure drop is considered ruptured. Upon disassembly, the specimens are leak-checked to locate the rupture to confirm the observation. All of the subsystems are connected by a single line to the primary pressure source. In this manner, one source station can service multiple specimens. In the case of this particular setup, the single station services 72 tests. Further improvements in rig fabrication allow one source to service as many as 250 specimens. Figure 8 shows an overall view of half the test facility. The two halves are back-to-back; the power console of the first rig can be seen in the upper right of the figure. The test facility is placed in the center of the room, allowing a technician to monitor the tests easily.

The specimens are loaded in the following manner: A portable vacuum station is connected to each test rig, and the retort and the specimens are evacuated during the period that the specimens are brought to temperature. After the temperatures have stabilized to within ±3°F, the retorts are backfilled with helium. During this period, the vacuum in the specimens is maintained. The valve to a specimen to be pressurized is then opened to the main pressure line. The gas from the main helium supply is then bled through a drying trap and through the standard gage.* When the required pressure has been maintained for ten minutes, the specimen monitor gage is checked and that pressure noted. The valve from the main pressure line to the specimen is then closed. The test time begins when the standardized gage indicates the required pressure. The remaining specimens are then pressurized in the same manner. To maintain isolation of each specimen once the tests have begun, the valves to individual specimens are opened one at a time.

4. Problem Areas

The test facility proved to be satisfactory during this test series, withstanding thermal and pressure cycling without difficulty.

One difficulty occurred with specimens during testing — some of the transition joints began to leak after a few hundred hours at 950°F. The maximum test

*Calibration traceable to NBS.

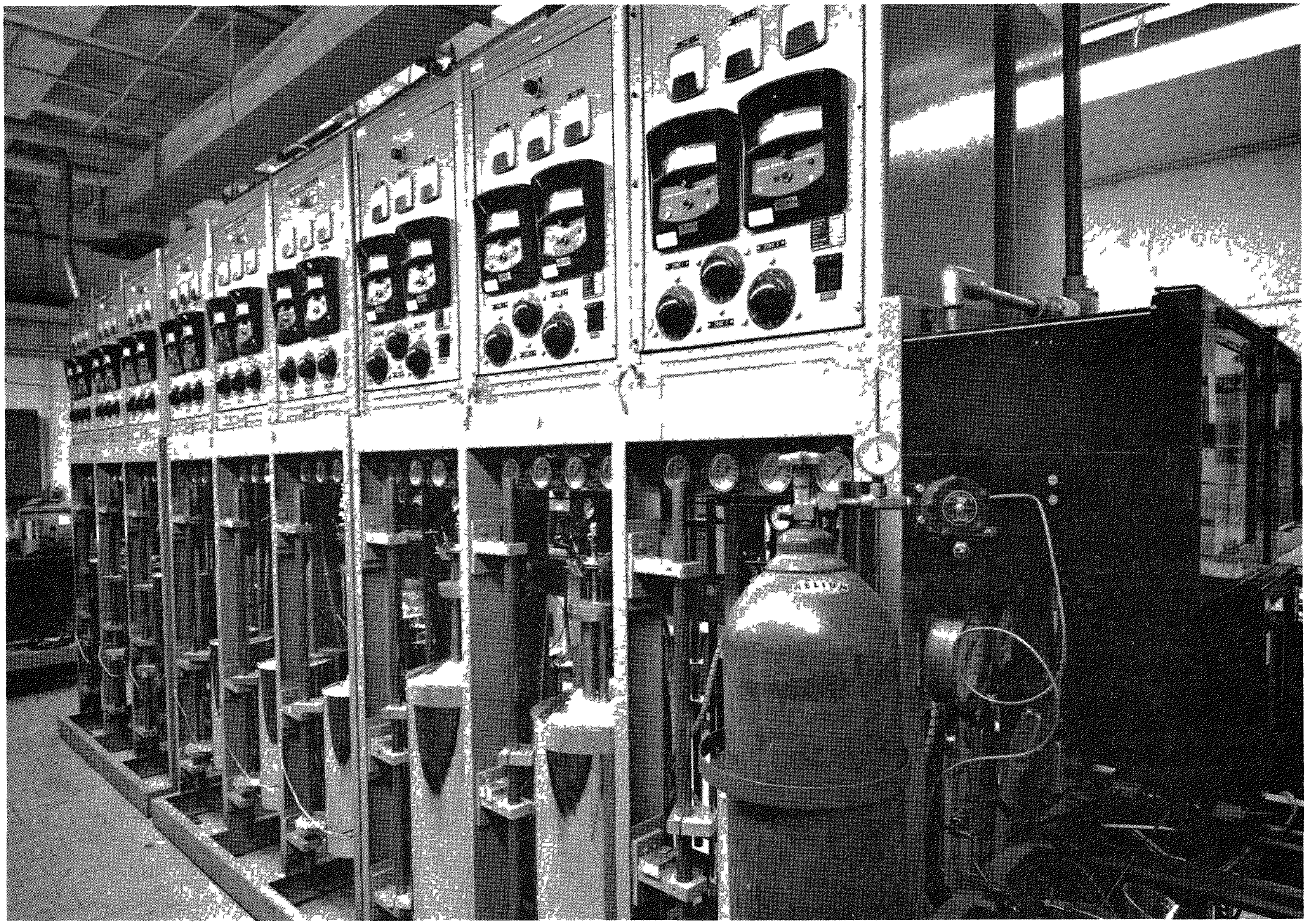

4 29 66 UNC

7680 1852

Figure 8. Test Bank

temperature (of additional specimens) was then reduced to 900°F until the problem could be solved. Examination of the joints indicated that the diffusion barrier had cracked and the aluminum had diffused into the steel. Subsequent development of the fabrication process has reduced the effects of this problem to an acceptable level. The problem is associated with the steel aluminum joints only; the test rigs have proven capability with nickel and steel wrought alloy to temperatures in excess of 1300°F.

# III. TEST RESULTS

The Mark III system was utilized to perform stress-rupture tests of finned tubing in an effort to determine a Larson-Miller type relationship between stress, time-to-rupture, and temperature. Four alloys were tested at four temperatures for a variety of internal pressures. The parameters of the test program are presented in Table 3. The results of the tests are presented in Table 4.

TABLE 3

PARAMETERS OF TEST PROGRAM

| | |
|---|---|
| Alloys | XAP 001, XAP 005, SAP 895, SAP 930 |
| Stress (psi) | 3100 to 6940 |
| Temperature (°F) | 750, 850, 900, 950 |

Under the conditions of the short-term burst tests by Ferry and Anderson,[4] the effect of the fins on the stress-rupture properties could not be detected. On the basis of their tests, the thin-wall formula $\sigma = PD/2t$ was apparently valid for a finned tube. For the purposes of evaluating stresses in this experiment, the thin-wall formula was consistently used. Further analytical and experimental work will be required to establish the actual relationship between geometry, pressure, and stress. That further work is needed is indicated by the fact that all tubing failures in this test series occurred in the fillet of the fin.

Material evaluations were performed to relate hoop stress to the Larson-Miller type parameter, which is a function of rupture time, temperature, and the material. The results of the Larson-Miller type evaluations are tabulated in Tables 5 and 6 and are illustrated in Figures 9 through 12. The methods used in evaluating the Larson-Miller material constants and equations are outlined in Appendix A. Appendix B details the author's comments pertaining to these evaluations.

The results of the Larson-Miller material constant ($C_B$) evaluations are tabulated in Table 5. This tabulation includes an evaluation number, the

# TABLE 4

## HOOP STRESS - TO - RUPTURE TIME DATA

| Type Material | Hoop Stress (psi) | Temperature (°R) | Rupture Time (hr) |
|---|---|---|---|
| XAP 001 | 6075 | 1210 | 3076 |
| | 6075 | 1210 | 1503 |
| | 6430 | 1210 | 2660 |
| | 6430 | 1210 | 1118 |
| | 6430 | 1210 | 3288 |
| | 4650 | 1310 | 516 |
| | 4650 | 1310 | 634 |
| | 4650 | 1310 | 1357 |
| | 4650 | 1310 | 876 |
| | 4650 | 1310 | 999 |
| | 4950 | 1310 | 371 |
| | 4950 | 1310 | 83 |
| | 5010 | 1310 | 800 |
| | 5290 | 1310 | 21.5 |
| | 5290 | 1310 | 12 |
| | 3800 | 1360 | 35 |
| | 3300 | 1410 | 35 |
| | 3500 | 1410 | 119 |
| | 3500 | 1410 | 85 |
| | 3500 | 1410 | 4 |
| | 3500 | 1410 | 32 |
| | 3600 | 1410 | 38 |
| | 3600 | 1410 | 78 |
| | 3810 | 1410 | 27 |
| | 3810 | 1410 | 105 |
| | 4125 | 1410 | 12 |
| XAP 001 | 4125 | 1410 | 12 |
| XAP 005 | 6075 | 1210 | 38 |
| | 6075 | 1210 | 744 |
| | 6430 | 1210 | 14 |
| | 6430 | 1210 | 1643 |
| | 4400 | 1310 | 371 |
| | 4400 | 1310 | 1343 |
| | 4950 | 1310 | 129 |
| | 4950 | 1310 | 4.25 |
| | 5010 | 1310 | 23.75 |
| | 3100 | 1360 | 875 |
| | 3500 | 1360 | 639 |
| | 3100 | 1410 | 83 |
| | 3250 | 1410 | 2 |
| | 3250 | 1410 | 5 |
| | 3310 | 1410 | 77.5 |
| | 3410 | 1410 | 37 |
| | 3810 | 1410 | 25 |
| | 4910 | 1410 | 0.75 |
| XAP 005 | 4910 | 1410 | 0.75 |

| Type Material | Hoop Stress (psi) | Temperature (°R) | Rupture Time (hr) |
|---|---|---|---|
| SAP 930 | 4650 | 1310 | 592 |
| | 4650 | 1310 | 551 |
| | 4650 | 1310 | 539 |
| | 3450 | 1360 | 591 |
| | 3800 | 1360 | 303 |
| | 3300 | 1410 | 297 |
| | 3500 | 1410 | 83 |
| | 3500 | 1410 | 61 |
| | 3810 | 1410 | 3 |
| SAP 930 | 3810 | 1410 | 26 |
| SAP 895 | 6710 | 1210 | 1178 |
| | 6940 | 1210 | 1525 |
| | 6940 | 1210 | 2331 |
| | 5440 | 1310 | 1407 |
| | 5500 | 1310 | 35 |
| | 5500 | 1310 | 1 |
| | 5620 | 1310 | 543 |
| | 4450 | 1360 | 272 |
| | 4800 | 1360 | 395 |
| | 3700 | 1410 | 322 |
| | 4275 | 1410 | 52 |
| | 5100 | 1410 | 10 |
| SAP 895 | 5100 | 1410 | 10 |

## TABLE 5

## TABULATION OF RESULTS OF LARSON-MILLER TYPE MATERIAL CONSTANT ($C_B$) EVALUATIONS FOR SAP MATERIALS

| Evaluation No | Material Type | Data Source | Stress Type | $Al_2O_3$ Content (wt %) | $\hat{C}_B$ | Standard Deviation $(S_{C_B})$ | 95% Confidence Limits | |
|---|---|---|---|---|---|---|---|---|
| | | | | | | | Lower | Upper |
| 1 | XAP 001 | AI | Hoop | 5-8 | 84.4 | 35.9 | 14.4 | 154.4 |
| 2 | XAP 005 | AI | Hoop | 5-8 | 41.6 | 11.6 | 17.1 | 66.1 |
| 3 | SAP 930 | AI | Hoop | 5-8 | 48.1 | 15.2 | 12.2 | 84.0 |
| 4 | SAP 895 | AI | Hoop | 9-12 | 69.0 | 41.0 | -50.3 | 132.3 |

## TABLE 6

## TABULATION OF RESULTS OF LARSON-MILLER TYPE EQUATION EVALUATIONS FOR SAP MATERIALS

| Evaluation No. | Material Type | Stress Type | Regression Equations Constants | | Correlation Coefficient (r) | Coefficient of Determination ($r^2$) | Standard Deviation ($S_{y \cdot x}$) |
|---|---|---|---|---|---|---|---|
| | | | a | b | | | |
| 1 | XAP 001 | Hoop | 5.49487 | $-1.59456 \times 10^{-5}$ | -0.9683 | 0.9376 | 0.023750 |
| 2 | XAP 005 | Hoop | 5.58657 | $-3.37100 \times 10^{-5}$ | -0.9164 | 0.8398 | 0.046371 |
| 3 | SAP 930 | Hoop | 5.76864 | $-3.16696 \times 10^{-5}$ | -0.9500 | 0.9026 | 0.019213 |
| 4 | SAP 895 | Hoop | 5.16472 | $-1.52725 \times 10^{-5}$ | 0.9189 | 0.8443 | 0.033746 |

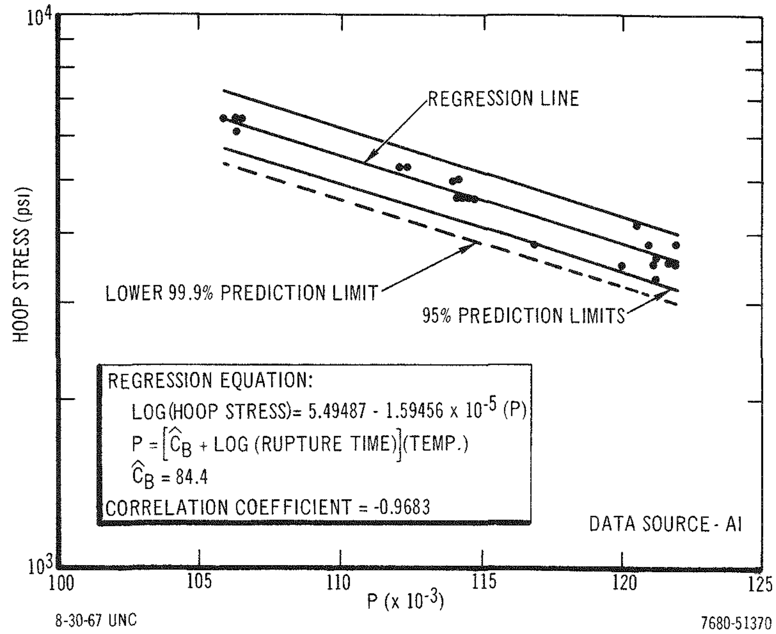


Figure 9. Larson-Miller Type Regression Evaluation for XAP 001

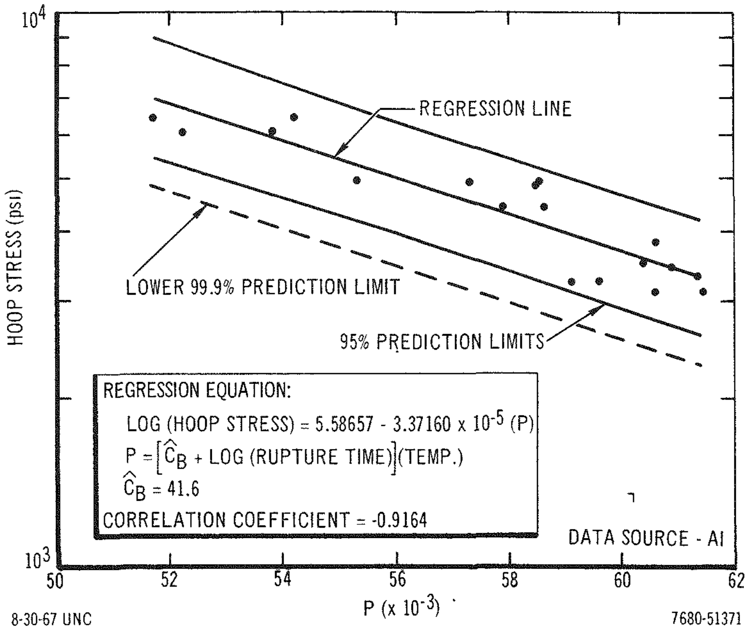


Figure 10. Larson-Miller Type Regression Evaluation for XAP 005

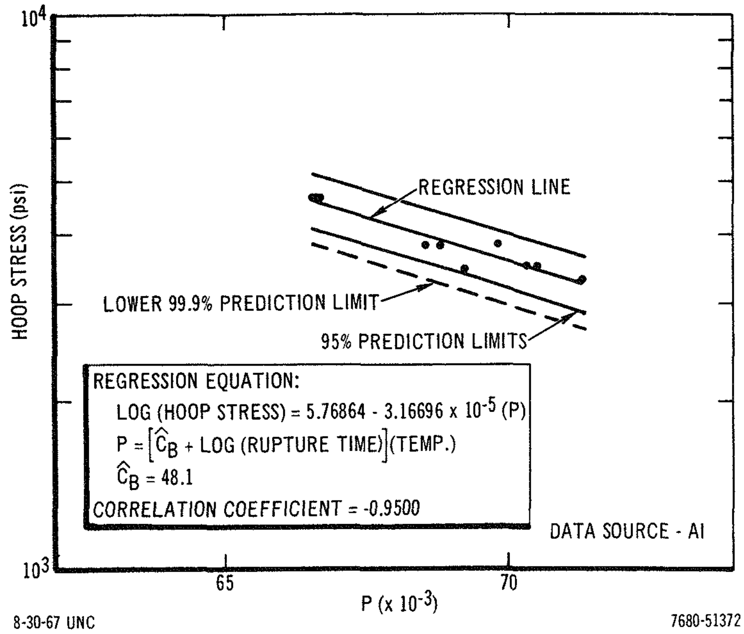


Figure 11. Larson-Miller Type Regression Evaluation for SAP 930

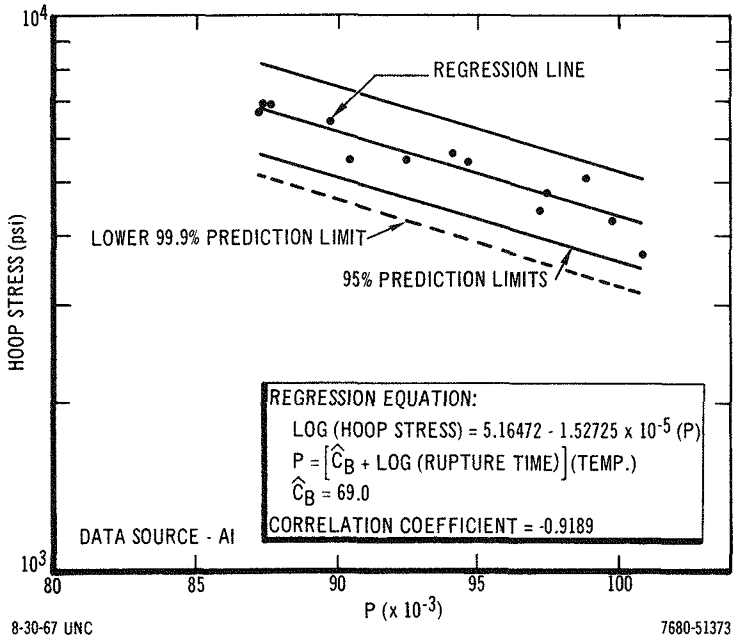


Figure 12. Larson-Miller Type Regression Evaluation for SAP 895

material type, test data source, type of stress, $Al_2O_3$ content (specified range), estimated material constant ($\widehat{C}_B$), and the standard deviation of the $C_B$ factor ($S_{C_B}$). The $C_B$ factor is a material constant that theoretically is independent of stress and represents the common point of intersection at $1/T = 0$ of extrapolated plots of log (rupture time) against 1/temperature for constant stress levels. The evaluations of these $C_B$ factors indicate relatively large standard deviations in relation to the magnitude of the estimated $C_B$ factors.

The results of the Larson-Miller type equation evaluations are tabulated in Table 6. This tabulation includes an evaluation number (which corresponds to the similar number in Table 5), the material type, type of stress, the constants from the estimated regression equations (a and b), correlation coefficient (r), coefficient of determination ($r^2$), and the standard deviation from the regression line ($S_{y \cdot x}$). The regression equation, for each evaluation, is in the form

$$\log(\sigma) = a + b\left[\widehat{C}_B + \log(t_r)\right] T$$

where the a and b values were determined from the linear least squares regression analysis, $\sigma$ is the stress level in psi, $t_r$ is rupture time in hours, $\widehat{C}_B$ is the estimated material constant (Table 5), and T is the temperature in degrees rankine. The value of the correlation coefficient is an indicator of how well the regression equation fits the data (i.e., $|r| = 1$ indicates a perfect fit of the regression line to the data; while, $r = 0$ indicates no dependency between the variables evaluated. A reasonable minimum correlation coefficient for good material property data would be $|r| = 0.9$. The sign of the correlation coefficient is the same as the sign of the slope of the regression equation). The coefficient of determination ($r^2$) is a measure of the amount of variation in the dependent variable (i.e., log stress — data points for Larson-Miller type evaluations) which is explained or accounted for by the regression equation. The standard deviation from the regression line ($S_{y \cdot x}$) is a measure of the variability of the dependent data values around the regression line. The relationship between $S_{y \cdot x}$ and the original variance ($S^2$) of the dependent variable is expressed by the equation,

$$S_{y \cdot x} = \left[(1 - r^2)S^2\right]^{1/2} \quad .$$

Figures 9 through 12 illustrate the results of the different Larson-Miller type evaluations. Each of these figures shows the calculated regression line with 95% prediction limits (i.e., limits within which 95% of the data points are expected to fall). Also shown on each chart are the associated data values where P, the Larson-Miller parameter, is expressed by the equation,

$$P = \left[\hat{C}_B + \log\ (t_r)\right]\ (T) \quad .$$

The 99.9% prediction limit has been drawn in for the lower side of the band.

An interpretation of one of these charts might be instructive. Assume that it is desired to determine the hoop stress which will rupture XAP 001 cladding in 100 hours (Figure 9) when tested at a temperature of 850°F (1310°R). The P factor for these conditions is [84.4 + log (100)] 1310 or $113.2 \times 10^3$. This P factor, based upon Figure 9, predicts that a stress level of 4900 psi will yield an average rupture time of 100 hours. However, the 95% prediction limits for this stress level range from $P = 110.0 \times 10^3$ to $P = 116.3 \times 10^3$. These P factors yield predicted rupture times for this stress level ranging to greater than 10,000 hours, illustrating that, while the prediction limits appear to be reasonably tight around the Larson-Miller type regression lines, these limits do in actuality encompass a very large range of possible rupture times.

Stress versus time-to-rupture plots of the SAP data are presented in Figures 13a, b, c, and d for the tests performed in the Mark III system. The slopes of curves for each alloy are characteristically flat, i.e., the slope approaches zero. Although this characteristic is troublesome when one tries to predict a time-to-rupture for a given stress, it has the advantage that once a minimum allowable stress is determined for a given temperature, the material will last well beyond the design life of a fuel element.

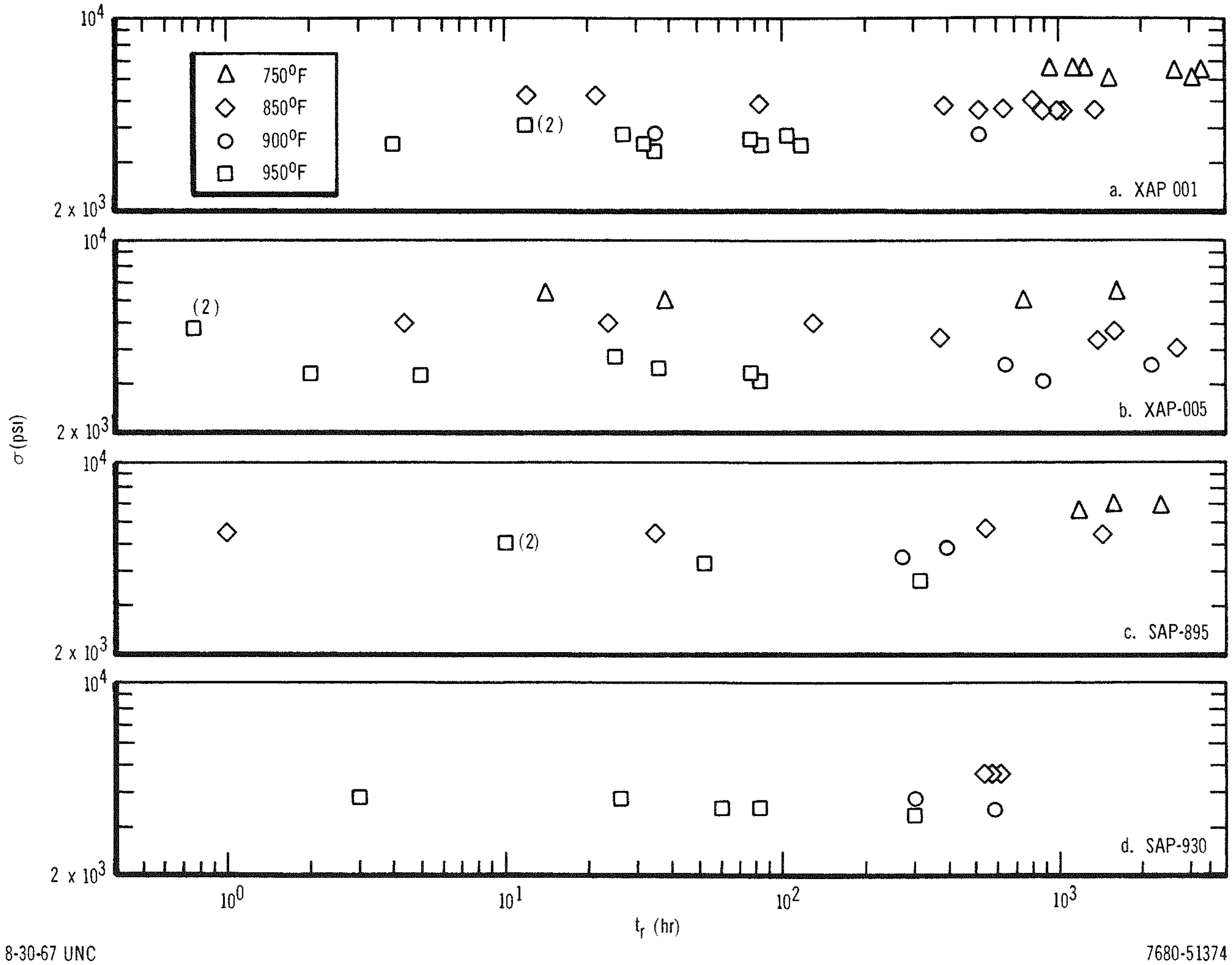


Figure 13. Stress Rupture for Biaxial Test Specimens

An attempt has been made to determine the stress below which one would expect less than one failure in a thousand specimens. To do this, a 99.9% prediction limit line was drawn on the low side of the Larson-Miller band for each alloy. The cladding life is assumed to be 13,210 hours (1-1/2 years) with a peak clad temperature of 850°F (1310°R). A value of P is calculated for each alloy utilizing the appropriate material constant ($C_B$). The resulting stresses are located on the lower 99.9% prediction limit for the alloys in Figures 9 through 12. The results are tabulated in Table 7. From this table it is seen that SAP 895 and XAP 001 are the stronger alloys.

TABLE 7

EXPECTED ALLOWABLE STRESSES FOR SINTERED ALUMINUM POWDER ALLOYS FOR 13210 HOURS AT 850°F (Unirradiated)

| Alloy Type | $\hat{C}_B$ | P | 3-σ Limit Stress (psi) |
|---|---|---|---|
| XAP 001 | 84.4 | $1.16 \times 10^5$ | 3650 |
| XAP 005 | 41.6 | $5.99 \times 10^4$ | 2500 |
| SAP 895 | 69.0 | $9.57 \times 10^4$ | 3650 |
| SAP 930 | 48.1 | $6.84 \times 10^4$ | 3250 |

## IV. CONCLUSIONS

The program has yielded significant stress-rupture information for finned tubing of SAP alloys operating in the temperature range of 750 to 950°F. The following conclusions have been reached:

a) Application of the Larson-Miller type analysis to the data shows that a wide disparity may exist in the material constant ($C_B$) for a given material (SAP 895) when it is tested at different sites. There also appears to be a dependency of this constant on the state-of-stress. There is a need for further investigation of this question, particularly to determine the effect of fins on the state-of-stress for long-time tube burst tests.

b) Application of the parameter to reactor operating conditions permits prediction of stresses that should result in no more than one failure for a thousand specimens.

## REFERENCES

1. D. J. C. Fleming, "Metallurgical Evaluations of SAP-895 Fuel Cladding Sheathing for WR-1 First Charge," DF65CAP 2 (1965)

2. G. E. Culley, "HWOCR Fuels Irradiation Test EXP-NRU-305," AI-CE-43 (September 15, 1967)

3. W. R. Jackson, "Development of Stainless Steel-Aluminum Transition Joint for High Temperature Service," AI-CE-72 (to be published)

4. P. B. Ferry and W. J. Anderson, "The Effect of Some Fabrication Variables on the Mechanical Properties of Sintered Aluminum Powder (SAP) Shapes," AI-CE-36 (August 15, 1967)

## APPENDIX A

The method used to determine the $C_B$ coefficient and the final Larson-Miller type equation involved two linear least squares regression evaluations. The first regression evaluation in each case was used to determine the $C_B$ coefficient while the second regression evaluation was used to determine the Larson-Miller equation.

The basic form of the Larson-Miller type equation is,

$$\log(\sigma) = A + B(P) \quad , \qquad \ldots(1)$$

where,

log = log base 10,

$\sigma$ = stress level (psi),

P = Larson-Miller parameter,

A = y intercept at P = 0, and

B = slope of equation.

The equation form of the Larson-Miller parameter (P) is,

$$P = [C_B + \log(t_r)](T) \quad , \qquad \ldots(2)$$

where,

$C_B$ = material constant,

$t_r$ = rupture time, and

T = temperature (°R)

Substituting Equation 2 into Equation 1 and expanding yields,

$$\log(\sigma) = A + BC_BT + BT\log(t_r) \quad . \qquad \ldots(3)$$

This equation can be estimated using linear least squares multiple regression analyses based upon the measured values of stress ($\sigma$), temperature (T), and rupture time ($t_r$) for a set of test data from a given material. The estimated equation will be in the form,

$$\log(\hat{\sigma}) = a + b_1 T + b_2 T \log(t_r) \quad , \qquad \ldots(4)$$

where $\log(\hat{\sigma})$ = predicted log of the stress level based upon a given temperature and rupture time. In this equation, $b_1$ is an estimate of the $BC_B$ factors in the second term of Equation 3, and $b_2$ is an estimate of the B factor in the third term in Equation 3. Therefore, $C_B$ can be estimated ($\hat{C}_B$) by $b_1/b_2$.

The final Larson-Miller type equation for each material evaluation was obtained using linear least squares regression analyses to estimate the following equation,

$$\log(\sigma) = A + B\,[\hat{C}_B + \log(t_r)]\,(T) \qquad \ldots(5)$$

where $\sigma$, $t_r$, and T are measured data values and $\hat{C}_B$ is the material constant estimated from the first regression evaluation.

The variances of the estimated $C_B$ factors are determined by assuming the $b_1$ and $b_2$ constants in Equation 4 are independent. With this assumption, the variances of a $C_B$ factor are estimated from the following equation,

$$V_{C_B} = \frac{b_1^2}{b_2^2}\left(\frac{V_{b_1}}{b_1^2} + \frac{V_{b_2}}{b_2^2}\right) \quad , \qquad \ldots(6)$$

where $V_{b_1}$ and $V_{b_2}$ are the variances (standard deviations squared) of the regression constants $b_1$ and $b_2$ (Equation 4), respectively. The standard deviation ($S_{C_B}$) of the estimated $C_B$ factor is determined by taking the square root of the estimated variance ($V_{C_B}$).

## APPENDIX B

The following observations are made in connection with the Larson-Miller type evaluations detailed in this report.

1) The Larson-Miller type equations are of the form that the dependent variable (rupture time) is used as an independent variable while the independent variable (stress level) is used as a dependent variable. This rearrangement of independent and dependent variables can result in a definite optimistic bias to the evaluation if the test data were obtained from a "normal" type material stress-rupture time testing program. To illustrate this effect, assume a very simple case of stress-rupture testing and data evaluation. Suppose six test specimens were tested at a constant temperature and two different stresses — three test specimens at each stress. Further, assume that the rupture times for stress Level 1, e.g., 1,000 psi, are 1,000, 3,162, and 10,000 hours while the rupture times for stress Level 2 — assume 10,000 psi — are 10, 31.62, and 100 hours.

To determine the normal Larson-Miller evaluation for these data, refer to Equation 3 of Appendix A. Since temperature is constant, the second term of Equation 3 can be combined with the first term because all factors in these two terms are constants. Also, the factors B and T of the third term can be combined into one term since both of these factors are constant. Therefore, the general form of the Larson-Miller type equation can be reduced to the simple linear equation form of,

$$\log(\text{stress}) = A + B\log(\text{rupture time}) \quad .$$

Therefore, using this equation form the linear least squares regression equation for these data is,

$$\log(\text{stress}) = 4.5714 - 0.4286\log(\text{rupture time}) \quad . \qquad \ldots(7)$$

The correct regression equation, which is unbiased, for these data, using stress level as the independent variable and rupture time as the dependent variable, is:

$$\log(\text{rupture time}) = 3.5000 - 2.0000\log(\text{stress level}) \quad . \qquad \ldots(8)$$

These data and equations are plotted on Figure 14. From this figure it can be seen that stress level required to yield a rupture time of $10^5$ hours based upon Equation 7 is 270 psi. This stress level predicts a rupture time of $4.3 \times 10^4$ hours based upon Equation 8 – the unbiased equation. Thus, the difference or bias, at this stress level, between the rupture times predicted from the unbiased regression equation (Equation 8) and the biased regression equation (Equation 7) is $5.7 \times 10^4$ hours or essentially a factor of 2 between the unbiased and biased predictions of rupture time. An important point to note in this example is the effect of extrapolation past the limits of the data (i.e., the greater the extrapolation the greater the absolute error and the factor of error between the correct and incorrect predictions of rupture time).

It is realized that in this type analysis the example used to illustrate the effect of rearranging the independent and dependent variables is somewhat over-simplified; but this example does show the effect of rearranging the independent and dependent variables where the data are obtained from the "normal" method of stress-rupture testing (i.e., testing multiple specimens to rupture at a few selected stress levels). The actual amount of

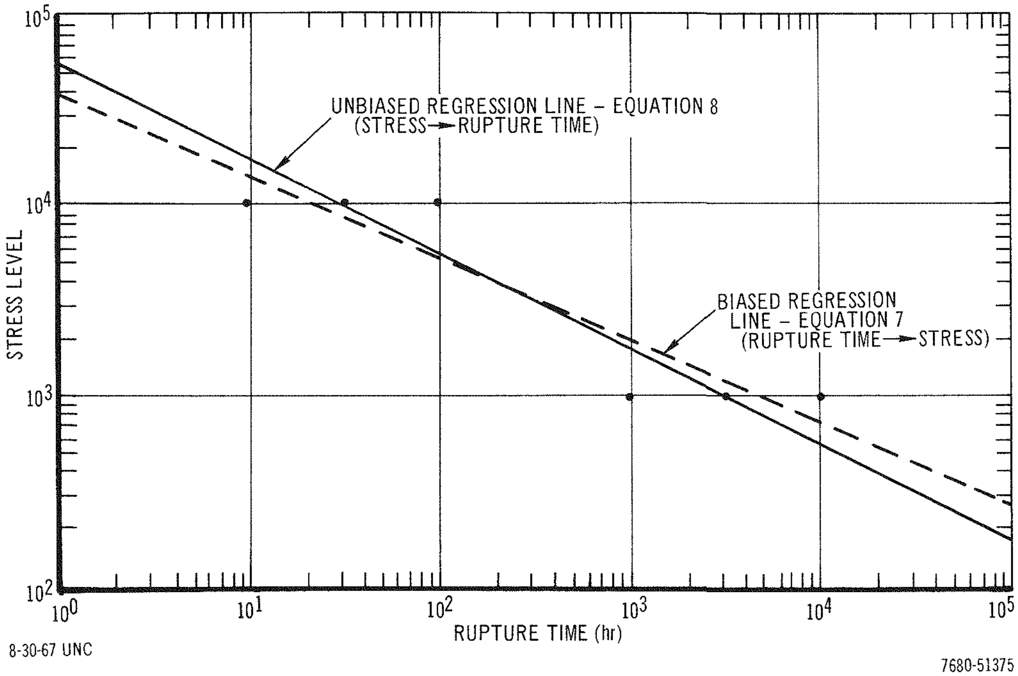


Figure 14. Effect of Rearrangement of Independent and Dependent Variables in a Stress - to - Rupture Time Regression Evaluation

bias derived from the rearrangement of variables, in any given evaluation is unpredictable, but is a function of (a) the degree of extrapolation past the limits of the data, (b) the number of stress levels from which data are obtained, (c) the total number of data points per stress level, and (d) the variability in the data for a given stress level. The recommended method of eliminating this type bias would be to derive an equation form for these types of evaluations which does not require the rearrangement of the independent and dependent variables.

2) The Larson-Miller type evaluations are of a linear form under the transformation to log base 10 of stress and rupture time data. The linear form for this equation might be correct for most materials. However, most of the plots of the data used in these evaluations indicate that a curvilinear form of equation might prove a significantly better fit to the data than does the linear equation. If this is true, the linear equations reported in this report provide optimistically biased estimates in the long rupture time regions of these equations, thereby potentially resulting in an under-designed, over-stressed piece of equipment. Therefore, it is recommended in future evaluations of this type that an equation form be derived which permits the evaluation of higher order terms (curvilinear terms). This evaluation should be of the type that permits the deletion of the higher order terms when the data evaluated are best described by a linear equation.

3) A third type of bias, which often enters into evaluations of stress-rupture data, is incurred when testing is terminated before rupture of the test specimen occurs. The termination of testing prior to rupture of the test specimen results in a truncation of the stress-to-rupture distribution. This truncation will result in a pessimistic bias in subsequent stress-to-rupture evaluations. This type bias is not as serious as the previously discussed biases in that this pessimistic bias will result in over-design, rather than under-design.